



TITLE:

Structural refinement and property optimization in an Fe-23Cr-8.5Ni duplex stainless steel

AUTHOR(S):

Xie, L.; Huang, T.L.; Wang, Y.H.; Zhang, L.; Wu, G.L.; Tsuji, N.; Huang, X.

CITATION:

Xie, L. ...[et al]. Structural refinement and property optimization in an Fe-23Cr-8.5Ni duplex stainless steel. IOP Conference Series: Materials Science and Engineering 2017, 219: 012045.

ISSUE DATE:

2017-08-01

URL:

<http://hdl.handle.net/2433/234990>

RIGHT:

Content from this work may be used under the terms of the Creative Commons Attribution 3.0 licence. Any further distribution of this work must maintain attribution to the author(s) and the title of the work, journal citation and DOI. Published under licence by IOP Publishing Ltd.

PAPER • OPEN ACCESS

Structural refinement and property optimization in an Fe-23Cr-8.5Ni duplex stainless steel

To cite this article: L. Xie *et al* 2017 *IOP Conf. Ser.: Mater. Sci. Eng.* **219** 012045

View the [article online](#) for updates and enhancements.

Related content

- [Research on damping properties optimization of variable-stiffness plate](#)
QI Wen-kai, YIN Xian-tao and SHEN Cheng
- [Ultrafine grained steels managing both high strength and ductility](#)
N Tsuji
- [Variability of Mechanical Properties and Weight for Reinforcing Bar Produced in Saudi Arabia](#)
F. Djavanroodi and A. Salman

**IOP | ebooks™**

Bringing you innovative digital publishing with leading voices to create your essential collection of books in STEM research.

Start exploring the collection - download the first chapter of every title for free.

Structural refinement and property optimization in an Fe-23Cr-8.5Ni duplex stainless steel

L. Xie¹, T.L. Huang¹, Y.H. Wang², L. Zhang¹, G.L. Wu^{1,*}, N. Tsuji³ and X. Huang⁴

¹ College of Materials Science and Engineering, Chongqing University, Chongqing 400045, China

² National Engineering Research Center for Equipment and Technology of Cold Strip Rolling, Yanshan University, Qinhuangdao 066004, China

³ Department of Materials Science and Engineering, Kyoto University, Kyoto 606-8501, Japan

⁴ Section for Materials Science and Advanced Characterization, Department of Wind Energy, Technical University of Denmark, DK-4000 Roskilde, Denmark

E-mail: wugl@cqu.edu.cn

Abstract. An Fe-23Cr-8.5Ni duplex stainless steel was used to prepare samples with different volume-fraction-weighted grain sizes ($d_{\alpha\gamma}$), ranging from the nano-scale to the micrometer-scale by cold rolling and subsequent annealing. The cold rolled sample with $d_{\alpha\gamma}$ of 72 nm showed a high yield strength of about 1.3 GPa but only a small tensile elongation. An abrupt increase of ductility was observed as $d_{\alpha\gamma}$ increased to 375 nm, resulting in a good combination of yield strength of 738 MPa and tensile elongation of 29%. Further increase of $d_{\alpha\gamma}$ up to the micrometer-scale results in continued decreases in yield strength but with only a limited improvement in the ductility.

1. Introduction

Nanostructured single phase metals produced by large strain deformation usually show a high ultimate tensile strength at a relatively small strain followed by a relatively large post elongation [1]. It is difficult to improve the limited ductility, especially the limited uniform elongation, until the grain size is increased up to the micrometer-scale, as widely observed in Al [2], Cu [3], Ti [4] and IF steel [5].

Several microstructural design principles have been put forward recently to improve the strain hardening ability of nanostructured metals, such as gradient structures [6], heterogeneous lamella structures [7] and dual or multi phases structures [8]. In this context dual-phase nanostructures also show a potential ability to achieve both high strength and good ductility. In the present study, we investigate the structural scale effect on the mechanical properties of a duplex stainless steel (DSS) with structural scales from nanometers to micrometers.



2. Materials and methods

The material used in the present study was an Fe-23Cr-8.5Ni DSS, with chemical composition of 0.001% C, <0.01% Si, <0.01% Mn, <0.001% P, <0.001% S, 8.52% Ni, 22.9% Cr, 0.002% N, 0.04% O, and the balance Fe (mass%). The ingot was homogenized at 1150°C for 2 h and hot forged at temperatures above 900°C. The hot forged plate was then cold rolled to a thickness reduction of 90% and subsequently annealed at temperatures from 700-1000°C for 5 min and 30 min in order to tailor the structure into different scales.

Microstructural characterization was carried out using an Axiovert 40 MAT optical microscope (OM) and a JEOL 2100 transmission electron microscope (TEM). The sampling plane was the longitudinal section containing the rolling direction (RD) and normal direction (ND). Samples for OM characterization were mechanically polished followed by electrochemical polishing in an electrolyte of 15 vol.% perchloric acid and 85 vol.% acetic acid at a voltage of 15 V at room temperature. Thin foils for TEM characterization were prepared by mechanical polishing to a thickness of 70 µm and then electropolishing using a twin-jet polisher in a solution of 25 vol.% perchloric acid and 75 vol.% ethanol at a voltage of 20 V at -20 °C. The volume fractions of constituent phases were quantified by X-ray diffraction (XRD) using a Rigaku D/max 2500PC X-ray diffractometer with Cu K α radiation and a step size of 0.02°. Tensile specimens of gauge dimensions 25 × 5 × 1 mm³ were machined from the cold rolled and annealed sheets with tensile axis along the RD, and tested at a uniaxial quasi-static strain rate of 6 × 10⁻⁴ s⁻¹.

Structural parameters in the DSS samples include grain size, phase size and volume fractions of the two phases. For simplification, we defined the structural size as the volume-fraction-weighted average grain size $d_{\alpha\gamma}$ [9], that is $d_{\alpha\gamma} = d_{\alpha}f_{\alpha} + d_{\gamma}f_{\gamma}$, where d_{α} and d_{γ} are the average grain sizes of the ferrite and austenite phases, respectively (determined by an intercept method along the ND) and where f_{α} and f_{γ} are the volume fractions of the two phases.

3. Results and Discussion

3.1. Microstructural characterization

Figure 1a shows the XRD spectra of the Fe-23Cr-8.5Ni DSS in the hot forged state and after cold rolling. Both ferrite and austenite diffraction peaks can be observed in the hot forged state. The volume fractions of the ferrite and austenite phases were determined to be 44.6% and 55.4%, respectively. After 90% cold rolling, the spectrum exhibits an absence of austenite, indicating the occurrence of a deformation-induced martensitic transformation. After annealing of the cold rolled sheet at 700°C or above, the deformation induced martensite (α' -martensite) transforms back to austenite. As shown in figure 1b, the austenite reversion is dependent on both the annealing temperature and the holding time. In the case of 5 min annealing, the α' -martensite gradually reverts to austenite, resulting in a slow increase of austenite fraction with temperature. The samples annealed for 30 min in the range from 700-1000 °C exhibit a large and almost constant austenite content, close to the amount of austenite in the hot forged state, indicating the completion of austenite reversion.

An example OM image of the 90% cold rolled sample is shown in figure 2a and reveals a microstructure consisting of alternating ferrite and α' -martensite lamellae, with dark and bright contrast, respectively. The samples annealed at 700 and 1000 °C for 5 min (figures 2b and 2c) both exhibit a banded structure similar to the cold rolled sample. Upon further annealing for 30 min, as shown in figures 2d and 2e, the microstructures change into a chain-like morphology.

The TEM image of the cold rolled sample shown in Figure 3a reveals a well-defined lamellar structure, with an average boundary spacing of 72 nm. After annealing at 700 °C for 5 min (figure 3b), recovery in ferrite and the reverse transformation from α' -martensite to austenite are initiated. The constituent phases in the TEM images were identified by electron diffraction. Some austenite grains are indicated by the white arrows and a diffraction pattern from the circled austenite grain is shown in the insert. The transformed austenite grains have an appearance similar to that of recrystallized austenite grains reported in austenitic stainless steels [11]. As the temperature is increased up to

1000°C, as shown in figure 3c, the austenite reversion continues by consumption of the remaining α' -martensite, and some austenite layers are well formed. The austenite layers consist of equiaxed grains, some of which contain annealing twins. In the ferrite phase, on the other hand, a typical recovered structure is seen. As the annealing time is extended to 30 min, as shown in figures 3d and 3e, further structural coarsening takes place. Table 1 lists the microstructural parameters of all samples investigated in the present experiment. It is seen that DSS samples with structural sizes ranging from 72 nm to 2.1 μm were obtained.

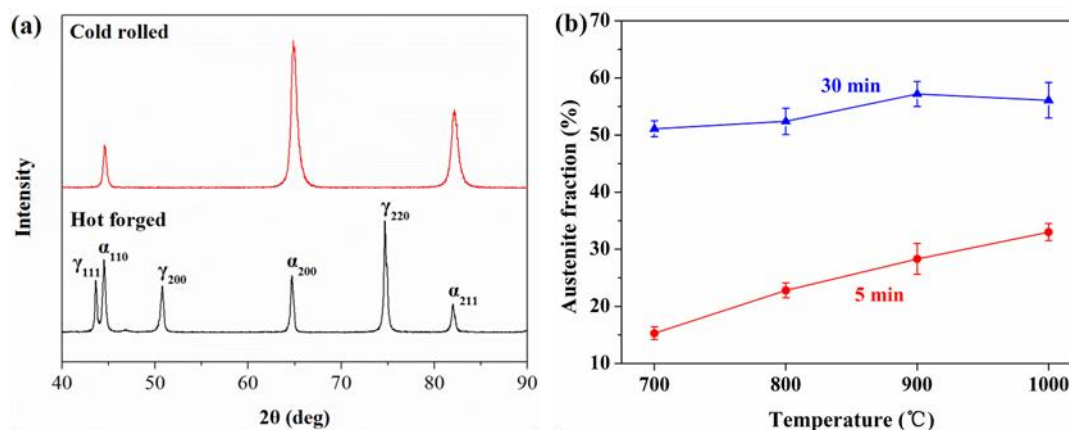


Figure 1. (a) XRD spectra of samples before and after 90% cold rolling. (b) Austenite fraction vs temperature for the cold rolled samples and then annealed at 700-1000°C for 5 and 30 min.

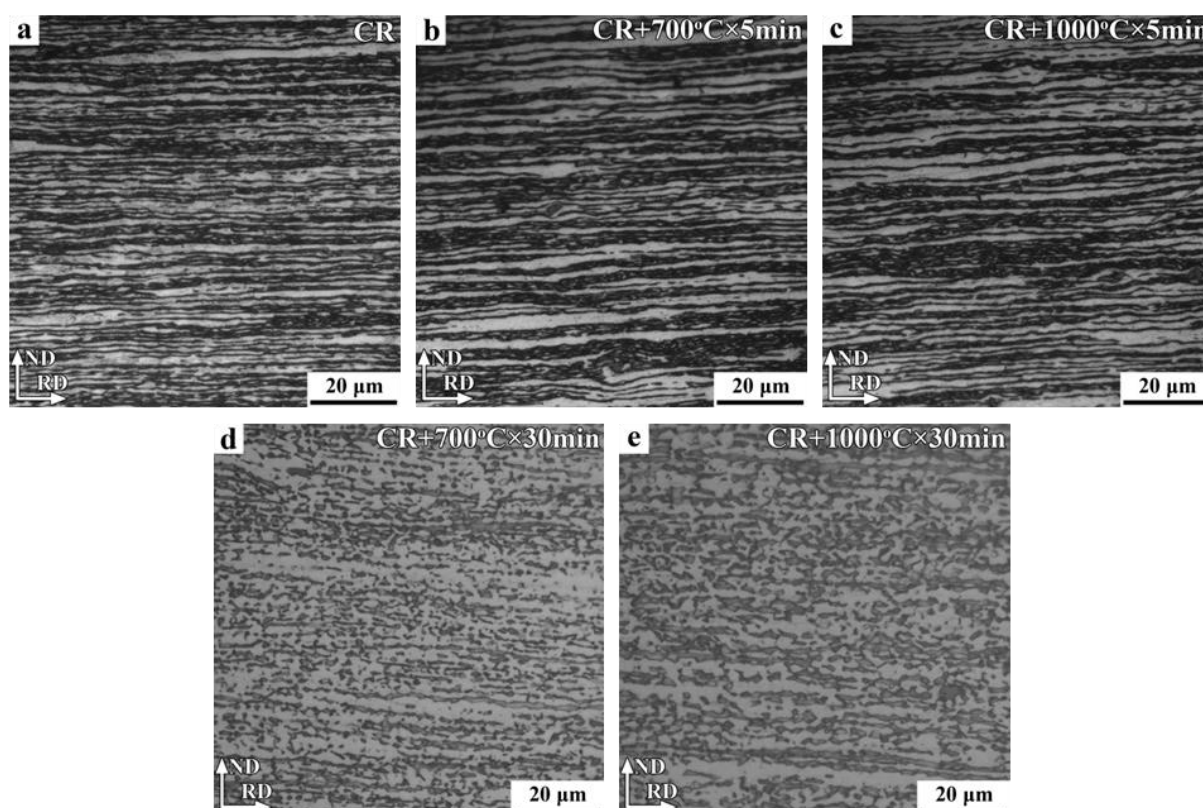


Figure 2. OM images of cold rolled and annealed samples: (a) cold rolled, (b) annealed at 700 °C for 5 min, (c) annealed at 1000 °C for 5 min, (d) annealed at 700 C for 30 min, (e) annealed at 1000 °C for 30 min.

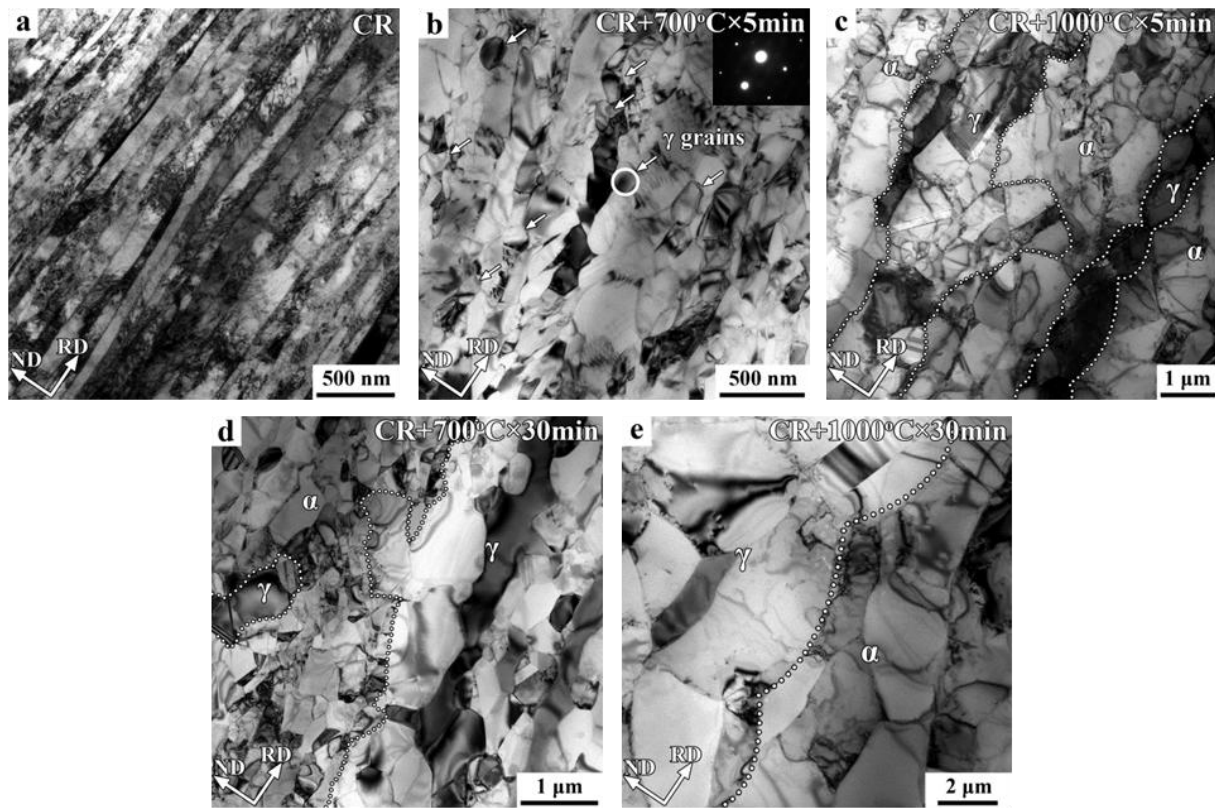


Figure 3. TEM images of cold rolled and annealed samples: (a) cold rolled, (b) annealed at 700°C for 5 min, (c) annealed at 1000°C for 5 min, (d) annealed at 700°C for 30 min, (e) annealed at 1000°C for 30 min.

Table 1. Microstructural parameters of cold rolled and annealed samples.

	$d_{\alpha\gamma}$	d_{α}	d_{γ}	f_{α}	f_{γ}
CR	72 nm	72 nm	—	100%	0%
CR+700°C×5min	169 nm	168 nm	172 nm	83.3%	16.7%
CR+800°C×5min	301 nm	294 nm	324 nm	77.2%	22.8%
CR+900°C×5min	571 nm	534 nm	665 nm	71.7%	28.3%
CR+1000°C×5min	808 nm	768 nm	890 nm	67.0%	33.0%
CR+700°C×30min	375 nm	347 nm	401 nm	48.9%	51.1%
CR+800°C×30min	723 nm	621 nm	817 nm	47.6%	52.4%
CR+900°C×30min	1.1 μm	1.1 μm	1.1 μm	42.8%	57.2%
CR+1000°C×30min	2.1 μm	1.8 μm	2.3 μm	43.9%	56.1%

3.2. Mechanical properties

Figure 4 shows the engineering stress-strain curves of the 90% cold rolled and annealed samples for volume-fraction-weighted grain sizes ($d_{\alpha\gamma}$) up to 2.1 μm. The cold rolled sample with $d_{\alpha\gamma}$ of 72 nm has a very high yield strength of about 1.3 GPa, but exhibits an ultimate tensile stress followed by necking at a very early stage of tensile deformation, resulting in a limited uniform elongation of less than 2% and a total elongation below 5%. As the volume-fraction-weighted grain size is increased to $d_{\alpha\gamma}$ = 169 nm, the yield strength rapidly decreases to 928 MPa, while the elongation shows almost no

increase. An abrupt increase of ductility is observed as $d_{\alpha\gamma}$ is increased to 375 nm. The yield strength under this condition is 738MPa with an elongation of 29%. As $d_{\alpha\gamma}$ is further increased the yield strength decreases gradually, but improvements in ductility are limited. A good combination of strength and ductility was therefore achieved in the sample with an average structural size of 375 nm. Under this condition the yield strength is 2.3 times higher than that of the sample with $d_{\alpha\gamma} = 2.1 \mu\text{m}$, while its tensile elongation (29%) is only a slightly smaller than that (33%) of the latter. Note that samples with $d_{\alpha\gamma}$ ranging from 375 to 808 nm exhibit a discontinuous yielding, characterized by a plateau (1~3% Lüders elongation) in the stress-strain curves. This was also observed in ultrafine grained single phase metals such as Al [2], Cu [3], IF steel [5] and austenitic stainless steels [11]. A continuous yielding is seen for structural sizes above 1 μm .

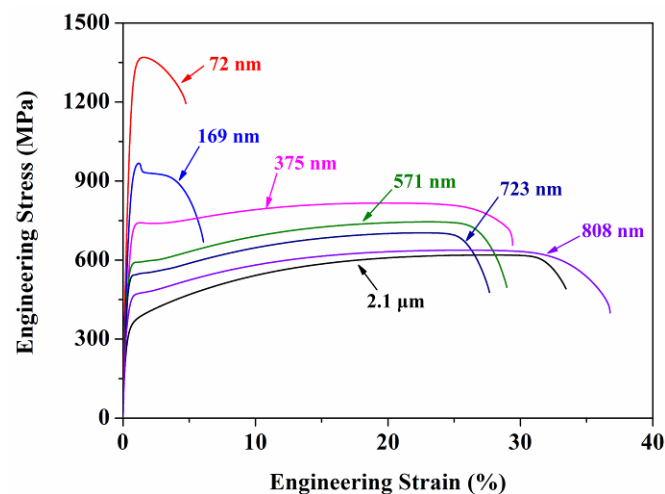


Figure 4. Engineering stress-strain curves of Fe-23Cr-8.5Ni DSS with a wide range of volume-fraction-weighted grain sizes.

It is interesting to observe that a significant increase in uniform elongation occurs at a structural scale of 375 nm. This is much finer than the scale where a similar transition is observed in single phase metals, which is often above a few micrometers. This observation can be attributed to the unique deformation characteristics of dual phase materials. For DSS, the plastic responses of individual phase to the applied strain are different from each other, resulting in a plastic strain gradient across phase interfaces [13]. This requires extra dislocations to be generated near the interfaces due to geometrical necessity, in order to make allow deformation compatibility [14, 15]. The geometrically necessary dislocations and their development with strain can lead to enhanced work hardening and tensile ductility.

4. Conclusions

Fe-23Cr-8.5Ni DSS samples with different structural sizes ranging from the nanometers to micrometers scale have been produced by cold rolling and subsequent annealing. The effect of structural size on the mechanical properties has been studied. The main results are summarized as follows:

- Cold rolling to 90% leads to a significant structural refinement down to 72 nm, which is associated with a high yield strength of about 1.3 GPa but a low tensile elongation of 5%.
- As the structural scale is increased by annealing to 375 nm, a rapid increase in elongation takes place, resulting in a good combination of yield strength and elongation, with values of 738 MPa and 29%, respectively.
- With further increase of the structural scale up to 2.1 μm , the yield strength gradually decreases, but the improvement in tensile elongation is limited.

Acknowledgments

The authors gratefully acknowledge the support from the National Natural Science Foundation of China (NSFC, Grant Nos.51471039, 51327805 and 51671039), and from the Fundamental Research Fund of Central Universities of China (Grant No. 106112017CDJPT130005).

References

- [1] Huang X 2009 *Scr. Mater.* **60** 1078-82
- [2] Tsuji N, Ito Y, Saito Y and Minamino Y 2002 *Scr. Mater.* **47** 893-9
- [3] An H, Wu S, Zhang Z, Figueiredo R B, Gao N and Langdon T G 2012 *Scr. Mater.* **66** 227-30
- [4] Li Z, Fu L, Fu B and Shan A 2013 *Mater. Lett.* **96** 1-4
- [5] Gao S, Chen M C, Joshi M, Shibata A and Tsuji N 2014 *J. Mater. Sci.* **49** 6536-42
- [6] Fang T H, Li W L, Tao N R and Lu K 2011 *Science* **331** 1587-90
- [7] Wu X L, Yang M X, Yuan F P, Wu G L, Wei Y J, Huang X and Zhu Y T 2015 *Proc. Natl. Acad. Sci. USA* **112** 14501-5
- [8] Koch C C, Scattergood R O and Murty K L 2007 *JOM* **59** 66-70
- [9] Fan Z Y, Tsakiroopoulos P and Miodownik A P 1992 *Mater. Sci. Technol.* **8** 922-9
- [10] Lee S J, Park Y M and Lee Y K 2009 *Mater. Sci. Eng. A* **519** 32-7
- [11] Saha R, Ueji R and Tsuji N 2013 *Scr. Mater.* **68** 813-6
- [12] Yu C Y, Kao P W and Chang C P 2005 *Acta Mater.* **53** 4019-28
- [13] Chen L, Yuan F P, Jiang P, Xie J and Wu X L 2014 *Mater. Sci. Eng. A* **618** 563-71
- [14] Ashby M F 1970 *Phil. Mag.* **21** 399-424
- [15] Mughrabi H 2001 *Mater. Sci. Eng. A* **317** 171-80